International Journal of Mechanical and Production Engineering Research and Development (IJMPERD)
ISSN (P): 2249-6890; ISSN (E): 2249-8001
Vol. 9, Issue 6, Dec 2019, 677–690

COMPUTATIONAL AND EXPERIMENTAL STUDIES OF CHARACTERISTICS OF THE FLOW DRAG, THROUGH DIMPLED SQUARE CYLINDERS

NASARUDDIN SALAM[1], RUSTAN TARAKKA[2], JALALUDDIN[3] & MUHAMMAD IHSAN[4]

[1]*Professor, Department of Mechanical Engineering, Hasanuddin University, Gowa, Indonesia*

[2,3]*Associate Professor, Department of Mechanical Engineering, Hasanuddin University, Gowa, Indonesia*

[4]*Lecturer, SekolahTinggiTeknikBaramuli, Pinrang, Indonesia*

ABSTRACT

Drag forces on hemispheric dimples in parallel and zigzag configuration on square cylindrical arethe focus of investigation and analysis in this paper. The research method has been carried out with a computer fluid dynamic (CFD) program using ANSYS FLUENT 18.0. The test piece has been made of acrylic in a total of 9 pieces with length of 300 mm, width 100 mm and height of 100 mm and dimpled ratio DR = 0.5. Dimples are arranged in rows, numbered from 1 to 8. All the specimens are treated in 7 equal flow velocity rates, ranging from 8 m/s to 20 m/s. The study which took place in laminar flow region with Reynolds number (Re) of 50064 to 125161 indicates that, the use of hemispherical dimples in both parallel and zigzag configurations reduces the drag coefficient (C_d). For example,in the same Re = 125161 the value of $C_d$on the plate without dimples was of 1.272, while on square cylinders with dimples in parallel configuration, the smallest drag coefficient, obtained on 2rows was of 1.203, and on dimpled square cylinder with zigzag configuration the smallest C_d was of 1.216, which was also on 2-rows configuration. Moreover, when compared with the square cylinder without dimples, the percentage of reduction drag coefficients are 4.396% and 5.412% for dimpled square cylinders in zigzag configuration and parallel configuration, respectively. The results show that the use of parallel configuration gives higher reduction than zigzag configuration.

KEYWORDS: Drag Coefficient, Reynolds Number, Dimpled Square Cylinder, Parallel & Zigzag Configuration

Received: Sep 07, 2019; **Accepted**: Sep 27, 2019; **Published**: Nov 15, 2019; **Paper Id**.: IJMPERDDEC201958

Original Article

1. INTRODUCTION

Various applications of dimpled square cylinder arrangement can be found on the surface of aircraft wing and on the surface of high-speed vehicles. “Computational and experimental analyses of dimpleeffect on aircraft wings have been conducted using NACA 0018 airfoils. Dimple shapes onsemi-spheres, hexagons, cylinders and squareshave been selected for the analyses, where airfoils haveparticularly been tested under the inlet velocity of 30m/s and 60m/s at different angle of attack (5˚, 10˚, 15˚, 20˚, and 25˚). The analysis favors the dimple effect by increasing L/D ratio and thereby providing the maximum aerodynamic efficiency, which provides anenhanced performance for the aircraft (Livya et al., 2015)”. The use of dimples on aircraft wings has shown the potentials to reduce pressure drag and the ability to delay flow separation (Baweja et al., 2016). Dimples application on spherical objects can reduce critical Reynolds number and can alter the separation point, further downstream (Aoki et al., 2012)”.

Dimpled surface with submicron roughness experiences surface hydrophobicity and decreasing skin friction by reducing shear stress on the wall, where drag is continuously reduced by about 3-5% (Paik et al.,

2015). Dimples with a single groove have proved to experience integration of the friction-wall coefficient in the direction of flow and have shown an increase in total drag up to 3.54% (Ranjan et al., 2011).

"The fluctuation of the pressure wall significantly increases near the trailing edge on the bump, where the boundary layer obtains a very adverse pressure gradient (Kim and Sung, 2006). Dimples configuration of 1.0 mm in diameter with dimpled ratio of 0.2, located on 30% - 60% and 75% - 95% of axial chord lengths on each side of suction have effectively reduced total pressure loss (Zhao et al., 2016). The characteristics of the turbulent boundary layer on the surface are influenced by the value of the Reynolds number, where friction factor on dimpled plates is higher on about 30% - 80% when compared to the plate without dimples (Zhou, et al., 2016)". If the spheresare embedded in the turbulent boundary layer, then the distribution of flow velocity fluctuations, flow line patterns, vorticity contours, flow velocity fields, turbulent kinetic energy and Reynolds stress correlations can be obtained using PIV data (Ozgoren et al., 2013).

Passive controls bydimplesin semi-spherical inward type on the plate, on a dimple ratio (RD) of 0.1 and a dimple depth equal to twice the thickness of the boundary layer, can cause instability and consequently create significant momentum transport. The shear layer is formed as the separation of flow across two dimpled lines. When vortex develops through a plate with several lines of dimpled configuration, the flow dynamics are disparate due to changes in momentum transport across the boundary layer (Beratlis et al., 2014). "From the analysis on the use of vortex generators to improve and control flow characteristics, dimples application were found to be useful (Lu et al., 2011; Storms, 1994). Further improvement has been proposed by incorporating the use of a novel surface modification in the form of dimples inspired by golf ball designs, which help to reduce the wake region induced by boundary layer separation (Bogdanović-Jovanović et al., 2012). From this experimental investigation, it has been observed that an airfoil with inward dimples has, in overall, the best performance, giving about approximately 16.43% increase in lift and approximately 46.66% of reduction in dragas compared to without dimpled airfoil, and it is giving the best lift/drag ratio. For inward dimpled airfoil, there is approximately 21.6% increase in lift to drag ratio (Mahamuni, 2015)".

The study shows that dimples produce lesser drag at positive angle of attacks with increase of lift(Prasath and Irish, 2017). Experimental results have shown the evidence for velocity 18 m/s and 33 m/s. As shown in graph, there is no flow separation occurs for both standard and dimpled airfoil models on the zero attack angle. As the attack angle increased from 0° to 5°, flow separation starts to initiate on the smooth surface airfoil model. As the attack angle increased from 5° to 10°, clear flow separation appeared on the upper surface. As the attack angle increased from 10° to 15°, clear flow separation appeared on the upper surface

"The main intention of aircraft aerodynamics is to develop the aerodynamic characteristics and maneuverability of the aircraft. The airfoil, which contains dimples will have comparatively a lesser amount of drag than the plain airfoil. Introducing dimples on the aircraft wing will create turbulence by creating vortices, which delays the boundary layer separation resulting in the reduction of pressure drag and increase of stall angles (Arunkumar et al., 2017)".

Computational fluid dynamics (CFD) simulations, investigating the passive drag reduction mechanism with the help of dents on flat plate have been performed(Ahirrao, 2016). From the comparisons of the C_d for all the dented plates, it was observed that the dented plate-1 had the least drag coefficient for these flow conditions among all the dented plate configurations. The C_d for dented plate-1 reduces as the flow velocity increases. Also, there is a sharp reduction in C_d from flow velocity 35 m/s to 40 m/s, an indication that there is a further potential to reduce the drag further. For the dented plate-7, Cd value decreases sharply from 5 m/s to 10 m/s, and then remains almost constant for the remaining flow conditions.

"Investigation of the streak lines has confirmed that the axis of the vortex contained within the dimples is oriented in the spanwise direction. The single row cases have resulted ina vortex, larger than the dimple itself. The vortex in this case acted as a bump, forcing the freestream flow around the dimple. The vortex has been observed to flow upstream creating a strong back flow region, directly behind the dimples. The multiple row case has resulted in a slightly different vortex geometry. The upstream dimple has a vortex, fully contained within the dimple. The region, directly behind the dimple at 65% of the axial chord has beenfully attached. The dimples at 76% of the axial chord have been observed to draw the flow downstream, thus forcing the upstream vortex to remain contained in the dimple(Casey, 2004)".

2. METHODOLOGY

Square cylindrical test pieceshave been added with dimples in parallel and zigzag configuration, on the top of the surface. "The treatment is to change the number of rows of dimples toward the x-axis (L_x/D) by 8 (eight) row variation levels (1, 2, 3, 4, 5, 6, 7 and 8), to set distances of dimples to z-axis (L_z/D) to be constant, to set dimpled ratio DR = 0.5 in hemispherical shapes. Each dimple sequence has been installed in parallel and zigzag configuration, then flowed in 7 equal flow velocity rates (U_0) of 8 m/s, 10 m/s, 12 m/s, 14 m/s, 16 m/s, 18 m/s and 20 m/s".

"The square cylindrical test materialshave beenmanufactured on 5 mm thick acrylic, while dimples have been formed by the help of CNC in dimensions of 300 mm length (L), 100 mm width (w) and 100 mm high (h)". Figure 1 shows square cylinder test model, (a) surface without dimples, (b) with the addition of dimple formations. Figure 2 shows dimple configuration in (a) zigzag configuration and (b) parallel configuration.

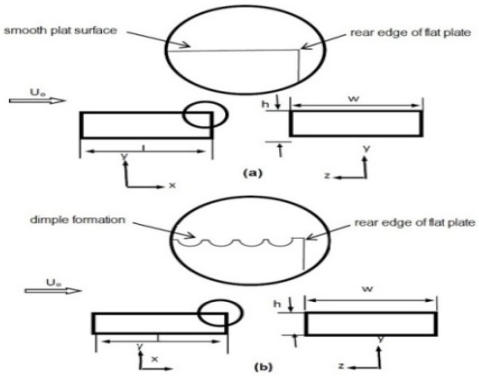

Figure 1: Square Cylinder Test Model, (a) Surface Without Dimples, (b) with the Addition of Dimple Formations.

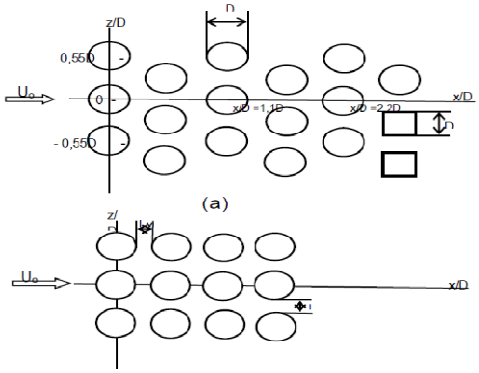

Figure 2: Dimple Configurations (a) Zigzag Configuration (b) Parallel Configuration.

Figure 3 depicts the position of dimples on the cylinder surface. As depicted in figure 2(a) and (b) the horizontal z-axis is perpendicular to the direction of flow.

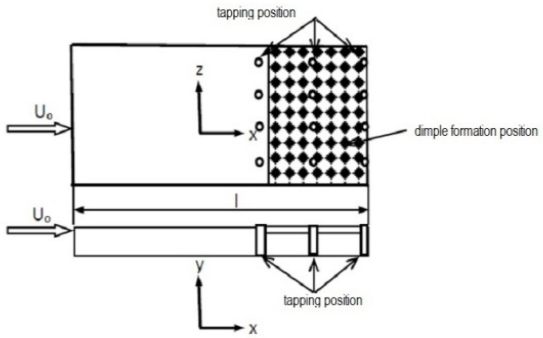

Figure 3: The Position of Dimples on the Cylinder Surface.

The distance between dimples on the x-axis (L_x) and the distance between dimples on the z-axis (L_z) are depicted in figure 3, which also shows the position of dimples on the surface of the square cylinder. Computational analysis using CFD simulation has beenbased on ANSYS FLUENT 18.0. The model of the test object is shown in figures 1–3. The simulation begins with the meshing process using ANSYS ICEM CFD 18.0 in automatic mode, where the software will determine the optimal meshing type according to geometry, generally using tetrahedrons. After the meshing process, the work then proceeded with the setup process in ANSYS FLUENT 18.0 consisting of the definition of the type of fluid, direction of fluid flow and fluid velocity at a speed of 20 m/s or at the Reynolds number (Re) = 125161. Subsequently, the number of iterations has been determined for 100 times and calculation processhasinitiated afterward. After performing the calculation process, the computational results in the form of pathline velocityhave been produced. One example of this type of meshing is shown in figure 4, below.

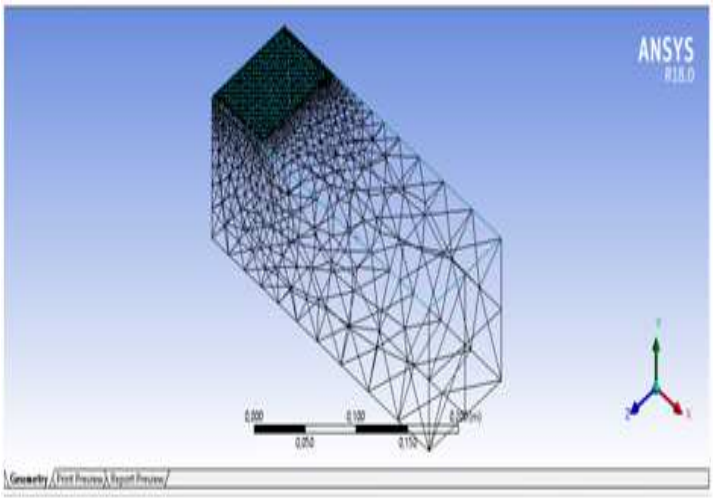

Figure 4: Meshing of Test Object with 8-rows Parallel Dimples Configuration.

"The experiment has been carried out using international standard testing equipment in the form of wind tunnel in the Laboratory of Fluid Mechanics, Department of Mechanical Engineering, Faculty of Engineering, Hasanuddin University. The 300 mm x 300 mm wind tunnel with the maximum airflow velocity through the test section is 20 m/s. To analyze the experimental data from the observation of drag force as well as to determine the flow characteristics of C_d, $(F_d)_{th}$ and Re due to the addition of the number of lines in each configuration, the following equations are used. Equation

(1) is used to determine the drag coefficient C_d where the actual or measured drag force $(F_d)_{act}$ and the theoretical drag force or air flow $(F_d)_{th}$ were obtained from Eq. (2), whereas ρ and A are the air density and sectional area of square cylinder. Determining the Reynolds number is conducted using Eq. (3), where U is the flow velocity across the test specimen and D is the square cylinder diameter (Olson and Wright, 1990)".

$$C_D = \frac{F_{d_{act}}}{F_{d_{th}}} \quad (1)$$

$$F_{d_{th}} = \frac{1}{2}\rho U^2 A \quad (2)$$

$$R_e = \frac{UD}{V} \quad (3)$$

The study has taken place in the laminar flow region, where Reynolds numbers calculated based on the square cylinder diameter are Re_D = 50064 to 125161.

3. RESULTS AND DISCUSSION

From computational analysis using CFD simulation, the following velocity pathline results are obtained. Figure 5 shows the velocity pathline for plate without dimples at a speed (U) of20 m/s. From figure 5, it can be seen that on the back of a square cylindrical model without dimples, the initial flow separation occurs on the back of the square cylinder. Similarly, the flow vortex is larger and lasts for a longer duration. Moreover, figure 6 shows the velocity pathlineson 1-rowdimple configurations at the similarvelocity of 20 m/s.

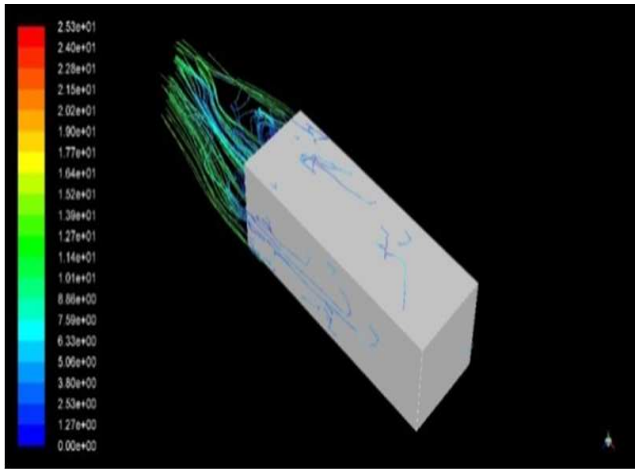

Figure 5: Velocity Pathline on a Square Cylinder Without Dimples at Flow Velocity 20 m/s.

It turns out that the flow vortex that occurs in 1-row configuration is smaller and lasts quite short, and the flow separation is slower when compared to the one without dimples. This shows that, the use of dimples on a square cylinder as a passive control can dampen the flow index and delay the flow separation.

Figures 6 and 8 show the comparison of the speed pathline in the parallel and zigzag configuration models, on the same number of dimpled lines, counted from 1 to 8, at speeds of 20 m/s.However, the velocity pathline displayed in the figures is only up to 3 (three) dimple rows, because the vortex pattern and flow separation from 3 lines up to 8 tend to increase, so that the lowest flow pattern is obtained in 2 rowsof dimples for all types of configurations (Salam et al., 2018).

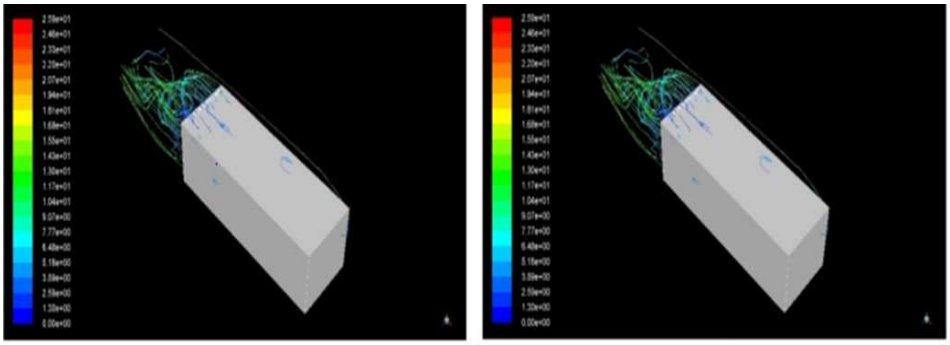

Figure 6: Velocity Pathline on Square Cylindersin for 1-row Dimplesin (a) Parallel Configuration and (b) Zigzag Configuration, Where Dimpled Ratio DR = 0.5 at Flow Velocity of 20 m/s.

The results of the comparison of these two configurations indicate that flow separation and flow processing are always smaller in parallel dimple configuration models when compared to that on zigzag dimple configurations. Specifically, when observed in 2-rows dimple formations as shown in figure 7, the comparison of flow and vortex after passing through a square cylinder, where in parallel configuration models, the vortex is smaller and faster to dissipate than the ones in the zigzag configuration model. Based on these characteristics, it can be concluded that, in parallel dimple configuration models, the passing fluid flow resistance is smaller than the one in zigzag dimple configurations.

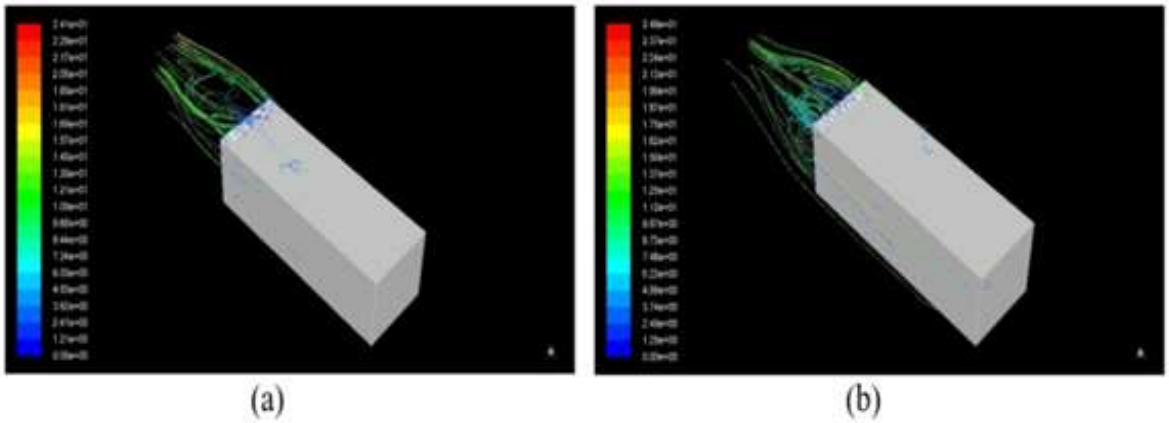

Figure 7: Pathline Speed on a Square Cylinder with a Dimpled Configuration of 2-Rows Dimple Formation in (a) Parallel Configuration and (b) Zigzag Configuration, Where Dimpled Ratio DR = 0.5 at Flow Velocity of 20 m/s.

Figure 8 shows an alteration in flow vortex which is greater than the one in the 2-rows dimple configuration. This phenomenon also shows a larger flow separation pattern, and this has resulted in a greater flow fluctuations, or conversely a larger flow fluctuation, resulting in greater flow vortices.This condition illustrates that 2-rows dimples configuration has more constraints than the 3-rowsdimples configuration. The phenomenon gives the same pattern for parallel and zigzag dimple configurations. However, the vortex flow in the zigzag dimples configuration is greater than the one on the parallel dimples configuration. The phenomena on 4-rows dimple configuration, wherevelocity pathline changes up to 8 lines are not shown in this article. Nevertheless, the growth pattern of velocity pathline shows an increase in flow vortex and earlier flow separation.

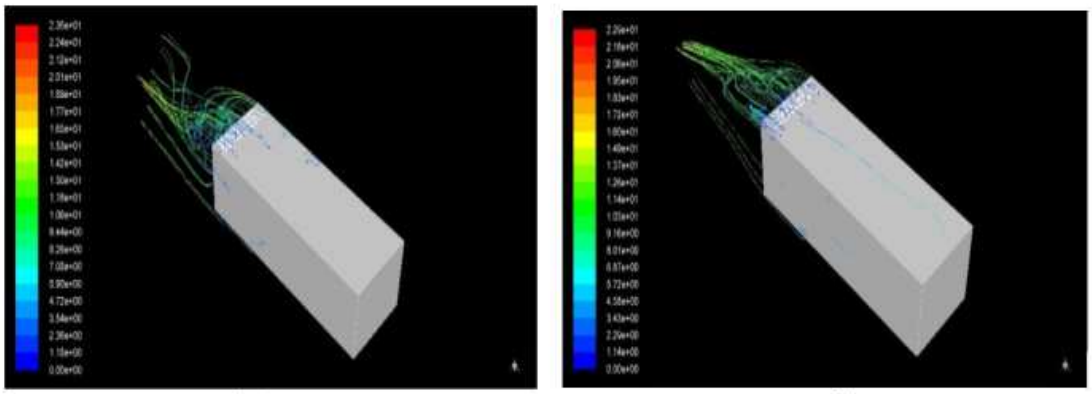

Figure 8: Pathline Speed on a Square Cylinder with Dimple Configuration of 3 Lines (a) Parallel and (b) Zigzag, with Dimple Ratio, DR = 0.5 at Flow Velocity 20 m/s.

This is because, the addition of the number of rowslarger than two rows is not able to reduce the shear stress on the wall. Instead of using 1-row dimple configuration and 2-rowdimple configuration, it is actually viable to reduce the shear stress on the wall when compared without dimples.The use of dimples on a square cylinder can lead to stability and instability, which causes significant momentum transport. The shear layer is formed, as the flow separation passes through the first two rows of dimples to become unstable and coherent collection of flow vortices.

From the experimental results of the airflow across the hemisphericallydimpled square cylinder in parallel configuration, it was obtained the actual resistance value $(F_d)_{act}$ of the airflow on the use of dimples with the number of rows (N), i.e. 1 to 8 rows and without dimples, 7 equal airflow velocity levels (U) from 8 m/s up to 20 m/s or at the number of Re = 50064 to 125161. Furthermore, the value is compared to the one of the theoretical resistance force $(F_d)_{th}$, and subsequently to drag coefficient (C_d) as shown in table 1.

Table 1: Drag Coefficient (Cd) for Parallel Configuration

Reynolds Number	Drag Coefficient (Cd)								
	Without Dimples	Number of Dimple Rows (N)							
		1	2	3	4	5	6	7	8
50064	1.451	1.397	1.251	1.262	1.289	1.315	1.342	1.369	1.396
62580	1.357	1.254	1.211	1.237	1.254	1.262	1.279	1.293	1.303
75097	1.344	1.261	1.227	1.241	1.260	1.265	1.287	1.300	1.311
87613	1.333	1.271	1.245	1.271	1.280	1.289	1.297	1.306	1.319
100129	1.322	1.295	1.268	1.282	1.289	1.295	1.302	1.309	1.324
112645	1.306	1.246	1.225	1.236	1.241	1.246	1.252	1.257	1.268
125161	1.272	1.220	1.203	1.220	1.224	1.233	1.237	1.241	1.254

Table 1 indicates that “the smallest drag coefficient of all levels of Reynolds number is on the use of 2-rows dimple formation. To examine the characteristic pattern of each level of Reynolds number, a graph of the relationship between the drag coefficient (C_d) and the number of rows (N) in the constant Reynolds (Re) number is developed as depicted in figure 9.The characteristic pattern in figure 9 shows that Reynolds number change does not affect the characteristic pattern of C_d to N, i.e. when N is enlarged, the C_d value is smaller. However, dimpled square cylinder with 2rows has a turning point, so for all levels of Reynolds numbers, the smallest value of C_d is obtained on N = 2 rows. This shows that atN = 2 rows, the flow wake at the back of the square cylinder is smallest, resulting in the smallest flow separation”.

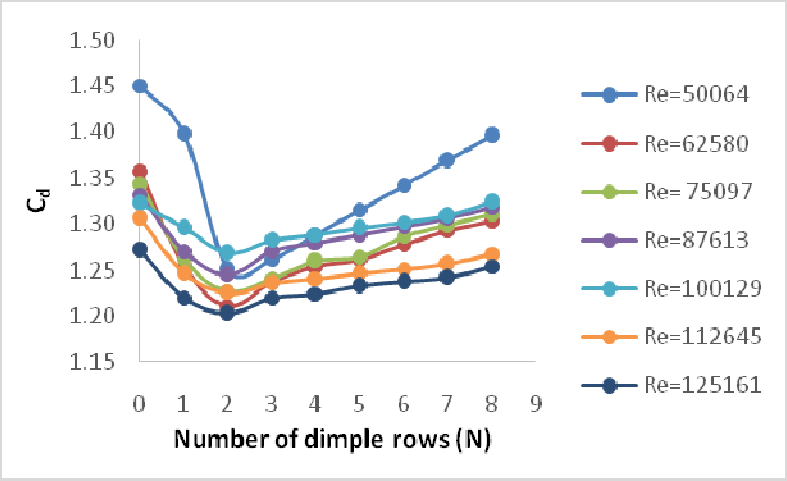

Figure 9: Relation Between Drag Coefficients with the Number of Rows of Parallel Dimple Configuration at the 7 Equal Levels of Reynolds Number (Re)

An interesting fact is notable on the 4-rows dimple formations, where the C_d values tend to be constant for any given Reynolds numbers. "This phenomenon shows that large number of dimpled rows is not able to delay the flow separation, so the value of C_d is just slightly higher when compared to the one without dimples. The characteristic pattern of this change of drag coefficient follows the pattern of objects disturbed in the tandem composed in rectangular cylinders where the exact interference position will decrease the flow drag coefficient on tandem bodies (Salam et al., 2017)".

"The same treatment is given on hemispherical dimpled square cylinder in zigzag configuration, which is obtained by the actual drag value $(F_d)_{act}$ of the airflow in the application of dimples with the number of rows (N) of 1 to 8 rows and without dimples, by treatments with 7 equal levels of airflow velocity (U) i.e. 8 m/s up to 20 m/s or on the Reynolds numbers of Re = 50064 to 12,161. Furthermore, the values are compared to the value of the theoretical drag force $(F_d)_{th}$. The value of the drag coefficient (C_d) is shown in table 2".

Table 2 shows that "the smallest drag coefficient of all levels of Reynolds numbers is obtained by the use of 2-rows formation. Based on these results, it is shown that zigzag dimpled configuration does not significantly detract the coefficient of drag, because on 2-rows formation, the configuration is not really zigzag".

Table 2: Drag Coefficients (Cd) for Zigzag Configuration

Reynolds Number	Drag Coefficient (Cd)								
	Without Dimples	Number of Dimple Rows (N)							
		1	2	3	4	5	6	7	8
50064	1.451	1.420	1.306	1.320	1.337	1.353	1.380	1.407	1.421
62580	1.357	1.289	1.254	1.272	1.275	1.283	1.293	1.300	1.312
75097	1.344	1.295	1.261	1.275	1.280	1.289	1.301	1.311	1.318
87613	1.333	1.300	1.267	1.280	1.289	1.297	1.305	1.315	1.324
100129	1.322	1.309	1.278	1.289	1.295	1.302	1.310	1.319	1.329
112645	1.306	1.257	1.230	1.246	1.252	1.257	1.262	1.267	1.273
125161	1.272	1.233	1.216	1.224	1.233	1.241	1.250	1.254	1.263

To examine the characteristic pattern of each level of Reynolds number, a graph of the relationship between the drag coefficient (C_d) and the number of rows (N) in the constant Reynolds number (Re) is developed, as shown in figure 10.

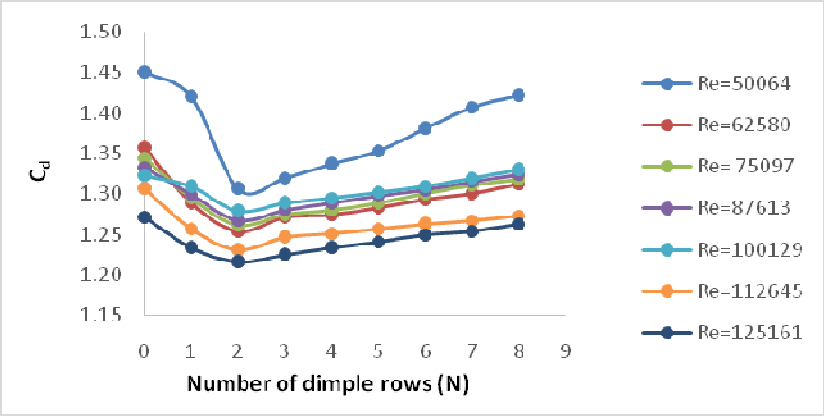

Figure 10: "Relationship Between Drag Coefficients with Number of Dimple Rows in Zigzag Configuration at the 7 Equal Levels of Reynolds Number".

The characteristic pattern in figure 10 shows "that Reynolds number alteration does not affect the characteristic pattern of C_d to N, i.e. when N is enlarged, the C_d value is smaller. However, dimpled square cylinder with 2 rows has a turning point, so for all levels of Re, the smallest value of C_d is obtained on N = 2 rows. This shows that at N = 2 rows, the flow wake at the back of the square cylinder is smallest, resulting in the smallest flow separation. Another interesting finding is that on the number of lines dimpled by 4, the C_d value tends to be constant for each Reynolds number level. This phenomenon shows that when the number of dimpled lines is added and then a zigzag configuration is formed, the delay the flow separation could not be achieved, so the value of Cd tends to be the same compared to that without dimples. The characteristic pattern of this drag coefficient change follows the pattern on parallel configuration pattern, but the flow separation occurred earlier in zigzag configuration".

Figure 11 below shows a comparison of the characteristics of dimpled parallel configurations and zigzag configurations, at 3 levels of the Reynods number (Re). The characteristic pattern in figure 11 shows that the change in the Reynolds number does not affect the characteristic pattern of the drag coefficient (C_d) on the number of rows (N). The largest C_d value is obtained on the square cylinder without dimples, when the number of N increases, the value of C_d decreases to 2 dimple rows, and after 2 lines up to 8 lines C_d increases.

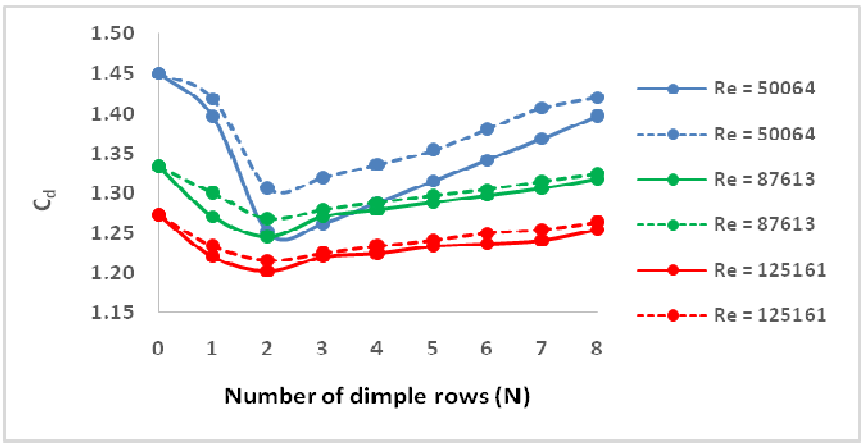

Figure 11: "Relationship Between Drag Coefficients with the Number of Rows Dimpled Parallel and Zigzag Configuration at 3 Levels of the Same Reynolds Number. The Value of Parallel Configuration is Shown in Continuous Lines While its Zigzag Counterpartis Shown Dashed Lines".

This shows the same characteristic pattern, both for parallel parallel configuration and zigzag configuration at all three Reynolds number levels. However, at Re = 50064, the decrease in the value of C_d was greater than that of Re = 87163 and Re = 125161. The characteristic pattern shown in figure 11 is the same as the velocity pathline characteristic pattern, as the results of computational simulation analysis in figures 5 to 8. This shows that, the wake of flow in the back of the dimpled square cylinder in parallel configuration is smaller than that of dimpled plate in zigzag configuration because the flow separation is more delayed.

This phenomenon shows that on 2-rows zigzag configuration, drag coefficient is equal to the one on 2-rows parallel configuration or in other words; the number of row on parallel configuration is added to form zigzag configuration. At Re = 125161 the smallest C_d value for dimpled square cylinder in 2-rows zigzag configuration is 1.216, while for dimpled square cylinder in 2 rows parallel configuration C_d value is 1.203. When the result is compared to square cylinder without dimples (C_d = 1.2715), the smallest drag coefficient percentage for zigzag configuration is 4.396%, while for parallel configuration, the drag coefficient is 5.411%. This result shows that the application of parallel configuration is better than the application of zigzag configuration. This result also shows that it is not necessary to install large numbers of rows of hemispherical dimples on the square cylinder where 2 rows are sufficient.

"Because in general, the use of square cylinder with dimple in zigzag or parallel configurations can be projected on a variety of objects, such as on the aircraft wings, vehicle bodies and blades on fluid machineries, based on the results of the research, the projection will also decrease the drag resistance, which is the main contribution of this research. Of the results of previous research as mentioned in the literature review in the introduction, none has applied dimple by giving effect of the number of lines to parallel and zigzag configuration, and compare the effect of both configurations which is the novelty of this research".

4. CONCLUSIONS

"From the analysis of fluid flow drag through the hemispherical dimpled square cylindrical in parallel and zigzag configuration, on the number of dimpled rows (N) from 1 to 8 and without dimples, with the wind tunnel inflows or outer sample flow (U) from 8 m/s to with 20 m/s or laminar flow which are on Reynolds number (Re) from 50064 to 125161, it can be concluded":

- "The larger the number of lines dimpled on the parallel configuration and zigzag configuration, the smaller the drag coefficient, but at N = 2 a turning point emerges or when N > 2 the drag coefficient is becoming larger".
- "The drag coefficient pattern tends to be the same for each dimple configuration change, flow speed or Reynolds number and the number of lines dimple. This phenomenon also shows that the use of dimples gives better results or the flow vortices are smaller and the flow separation is slower than without dimples".
- "The use of hemispherical dimpled parallel and zigzag configurations in high speed vehicles is very useful, because it can reduce fluid flow resistance".

ACKNOWLEDGEMENT

This research is financed by the Ministry of Research, Technology and Higher Education, the Republic of Indonesia, through the University Professorship Research Scheme (PPU) of Fiscal Year 2018, and to Head of Laboratory of Fluids Mechanics Department of Mechanical Engineering Faculty of Engineering,Hasanuddin University, on the permits and facilities provided in the implementation of this research.

REFERENCES

1. *Livya, E., Anitha, G., and Valli, P., Aerodynamic analysis of dimple effect on aircraft wing, World Academy of Science, Engineering and Technology, International Journal of Aerospace and Mechanical Engineering, Vol. 9, No. 2 (2015), pp. 350–353. https://doi.org/10.5281/zenodo.1099926*
2. *Baweja, C., Dhannarapu, R., Niroula, U., andPrakash, I., Analysis and optimization of dimpled surface modified for wing planforms, 7th International Conference on Mechanical and Aerospace Engineering, 2016. https://doi.org/10.1109/icmae.2016.7549590.*
3. *JK, S., Reddy, K. R., & Yellampalli, S. S. Design and implementation of fuel flow control unit for aero engine.*
4. *Aoki, K., Muto, K., and Okanaga, H., Mechanism of drag reduction by dimple structures on a sphere, Journal of Fluid Science and Technology, Vol. 7, No. 1, (2012), pp. 1–10. https://doi.org/10.1299/jfst.7.1.*
5. *Paik, B.G., Pyun, Y.S., Kim, K.Y., Jung, C. M., and Kim, C. G., Study on the micro-dimpled surface in terms of drag performance, Experimental Thermal and Fluid Science, Vol. 68 (2015), pp. 247–256.*

   https://doi.org/10.1016/j.expthermflusci.2015.04.021.
6. *Parameswari, M. Textile and dye industry effluent, sludge and amendments on dehydrogenase and phosphatase activity of soil under sunflower crop.*
7. *Ranjan, P., Paul, A. R., and Singh, A. P., Computational analysis of frictional drag over transverse grooved flat plates, International Journal of Engineering, Science and Technology, Vol. 3, No. 2 (2011), pp. 110–116. https://doi.org/10.4314/ijest.v3i2.68680.*
8. *Khan, S. A., Shahzer, M., Sultan, D., & Ali, R. Thermal and solutal buoyancy effects on mixing of opposed laminar jets in a two-dimensional passive mixer at a higher Reynolds number.*
9. *Kim, J., and Sung, H. J., Wall pressure fluctuations in a turbulent boundary layer over a bump, AIAA Journal, Vol. 44, No. 7 (2006), pp. 1393–1401. https://doi.org/10.2514/1.6519.*
10. *Zhao, Y., Lu, H., and Sun, Y., Experimental studies of dimpled surface effect on the performance of linear cascade under different incidence angles, Procedia CIRP 9th International Conference on Digital Enterprise Technology, Vol. 56 (2016), pp. 137–142. https://doi.org/10.1016/j.procir.2016.10.043.*
11. *Zhou, W., Rao, Y., and Hu, H., An experimental investigation on the characteristics of turbulent boundary layer flows over a dimpled surface, Journal of Fluids Engineering, Paper No. FE-15-1174, Vol. 138, No. 2 (2016), pp. 02120401–02120413. https://doi.org/10.1115/1.4031260*
12. *Deka, P., Naidu, K. R., Mandal, T. K., & Majumder, S. K. (2014). Flow pattern shifting and drag reduction in oil-water flow in pipe. International Journal of Research in Engineering & Technology, 2(2), 245–252.*
13. *Ozgoren, M., Okbaz, A., Dogan, S., Sahin, B., and Akilli, H., Investigation of flow characteristics around a sphere placed in a boundary layer over a flat plate, Experimental Thermal and Fluid Science, Vol. 44 (2013), pp. 62–74. https://doi.org/10.1016/j.expthermflusci.2012.05.014.*
14. *Beratlis, N., Balaras, E., and Squires, K., Effects of dimples on laminar boundary layers, Journal of Turbulence, Vol. 15, No. 9 (2014), pp. 611–627. https://doi.org/10.1080/14685248.2014.918270.*
15. *Lu, F., Li, Q., Shih, Y., Pierce, A, and Liu, C., Review of micro vortex generators in high speed flow, 49th AIAA Aerospace Sciences meeting including the New Horizons forum and Aerospace Exposition, January, (2011). https://doi.org/10.2514/6.2011-31.*

16. *Storms, B. L. and Jang, C.S., Lift enhancement of an aerofoil using a gurney flaps and vortex generators, Journal of Aircraft, Vol. 31, No. 3 (1994), pp. 542–547. https://doi.org/10.2514/3.46528.*

17. *Bogdanović-Jovanović, J.B., Stamenković, Ž. M., and Kocić, M.M., Experimental and numerical investigation of flow around a sphere with diples for various flow regimes, Thermal Science, Vol. 16, No. 4 (2012), pp. 1013–102. https://doi.org/10.2298/tsci120412115b.*

18. *Mahamuni, S.S., A review on study of aerodynamic characteristics of dimple effect on wing, International Journal of Aerospace and Mechanical Engineering, Vol. 2, No. 4 (2015), pp. 18–21.*

19. *Prasath, M.S., and Irish A.S., Effect of dimples on aircraft wing, GRD Journals – Global Research and Development Journal for Engineering, Vol. 2, No. (2017), pp. 234–241.*

20. *Arunkumar, A., Gowthaman, T.S., Muthuraj, R., Vinothkumar, S., and Balaji, K., Numerical investigation over dimpled wings of an aircraft, International Journal for Research in Applied Science & EngineeringTechnology (IJRASET), Vol. 5, No. 4 (2017), pp. 206–211. https://doi.org/10.22214/ijraset.2017.4041.*

21. *Ahirrao, H., Numerical investigation of drag reduction on flat plates using dents, International Journal of Innovative Research In Technology (IJIRT), Vol. 3, No. 2 (2016), pp. 14–19.*

22. *Casey, J. P., Effect of dimple pattern on the surpression of boundary layer separation on a low pressure turbine blade, Thesis, Air Force Institute Of Technology, Wright-Patterson Air Force Base, Ohio, (2004).*

23. *Olson, R. M., and Wright, S.J., Essentials of Engineering Fluid Mechanics, 5th Ed., (1990), Harper & Row.*

24. *Salam, N., Tarakka, R., Jalaluddin, and Bachmid, R., The effect of the addition of inlet disturbance body (IDB) to flow resistance through the square cylinders arranged in tandem, International Review of Mechanical Engineering (I.RE.M.E.), Vol. 11, No. 3 (2017), pp. 181–190. https://doi.org/10.15866/ireme.v11i3.11338.*

AUTHORS PROFILE

Mr. Nasaruddin Salam, born in Bulukumba on December 20th 1959 is a Professor and the Chairman of Fluid Mechanics Laboratory in Department of Mechanical Engineering, Faculty of Engineering, Hasanuddin University Makassar Indonesia. He graduated with Engineer Degree from Hasanuddin University where he also pursued his Master Degree in Mechanical Engineering. He holds a doctoral degree from Brawijaya University, Malang Indonesia. His research fields include fluid dynamics particularly on tandem bodies. Prof. Nasaruddin Salam is a member of the Institutions of Engineers Indonesia. He is currently the Secretary of Hasanuddin University. He previously served as the Vice Rector for Student Affairs at Hasanuddin University. Scopus ID 56402961600.

Mr. Rustan Tarakka, born in Pinrang on August 27th 1975. He is an Associate Professor of Mechanical Engineering, Faculty of Engineering, Hasanuddin University, Makassar, Indonesia. He graduated with Bachelor of Engineering Degree from Hasanuddin University where he also pursued his Master Degree in Mechanical Engineering. He holds a doctoral degree from University of Indonesia, Jakarta, Indonesia. His research areas are on fluid dynamics and computational fluid dynamics. Dr. Rustan is a member of the Institutions of Engineers Indonesia.Scopus ID 55178555400.

Mr. Jalaluddin, born in Sompu on August 25th 1972 obtained a Doctor of Engineering in Mechanical Engineering in 2012 from Saga University Japan. He graduated with Bachelor of Engineering Degree from Hasanuddin University. He is an Associate Professor of Mechanical Engineering of Hasanuddin University, Makassar, Indonesia. His area of research covers Ground Heat Exchanger for Space Conditioning System, Renewable Energy focus on Solar Energy including Solar Water Heating System and Photovoltaic Applications. Dr-Eng. Jalaluddin is a member of Institutions of Engineers Indonesia. Scopus ID 36571814200.

Mr. Muhammad Ihsan, born in Watampone, February 20th 1977, is a lecturer on Sekolah Tinggi Teknik Baramuli, Pinrang, Indonesia. He graduated from Hasanuddin University with a bachelor in engineering. He also holds master degrees in transport engineering from Asian Institute of Technology, Bangkok, Thailand and Universitas Gajah Mada, Yogyakarta, Indonesia. His research interests include transport engineering, fluid mechanics and hydraulics. Mr. Muhammad Ihsan is a member of Institutions of Engineers Indonesia. Scopus ID 57202436594.